Kinetics and Catalysis, Vol. 42, No. 6, 2001, pp. 837–846. Translated from Kinetika i Kataliz, Vol. 42, No. 6, 2001, pp. 917–927.
Original Russian Text Copyright © 2001 by Simonova, Barelko, Toktarev, Zaikovskii, Bukhtiyarov, Kaichev, Bal'zhinimaev.

Catalysts Based on Fiberglass Supports: III. Properties of Supported Metals (Pt and Pd) According to Electron-Microscopic and XPS Data

L. G. Simonova*, V. V. Barelko, A. V. Toktarev*, V. I. Zaikovskii*,**
V. I. Bukhtiyarov*, V. V. Kaichev*, and B. S. Bal'zhinimaev*
** Boreskov Institute of Catalysis, Siberian Division, Russian Academy of Sciences, Novosibirsk, 630090 Russia*
*** Institute of Problems of Chemical Physics, Russian Academy of Sciences, Chernogolovka, Moscow oblast, 142432 Russia*

Received March 13, 2000

Abstract—Under various preparation conditions, metals supported on leached borosilicate and soda–silica fiberglass form three types of particles. First, these are metal particles in sizes from tens to hundreds of angstrom distributed over the outer surface of fibers. Second, in the presence of mesopores in fiberglass supports (borosilicate glasses), metal particles of commensurable sizes (15–100 Å) are localized in the cavities. Third, dispersed (<10 Å) particles are present in the bulk of fiberglass; these particles are intercalated into the bulk of leached glasses as deep as several hundreds of angstrom. The amount of a metal and the depth of penetration into the bulk of fiberglass can be controlled by preparation conditions and by the addition of cointercalates, which are responsible for pillaring effects.

INTRODUCTION

Recently, it was found that catalytic systems based on leached fiberglass materials containing small amounts of metals (Pt, Pd, Ag, Cr, Co, etc.) are very promising. They can be used in many chemical processes (the oxidation of methane, propane, butane, ammonia, sulfur dioxide, and the hydrogenation of vegetable oils and aromatic nitro compounds), in which they are more active than commonly used supported catalysts [1–4]. It was suggested that this is due to the presence of specific active centers formed in the interaction of a metal with a glass [3]. The physicochemical properties of fiberglass-supported metals have not been studied in detail. Previously [5, 6], we examined the properties of fiberglass supports prepared by leaching soda–silica glass and alumina borosilicate glass. In this work, we used transmission electron microscopy (TEM) and X-ray photoelectron spectroscopy (XPS) for studying the morphological and electronic properties of metals (Pt and Pd) supported on fiberglass carriers prepared by leaching soda–silica glass and alumina borosilicate glass. The results of testing these catalysts in the reactions of sulfur dioxide oxidation, deep oxidation of *n*-butane and propane, and the selective hydrogenation of an ethylene–acetylene mixture will be presented in the subsequent papers.

EXPERIMENTAL

The following two types of fiberglass supports, which were described previously [5, 6], were used: soda–silica fiberglass leached at 90°C for 60 min (support CB; $S_{sp} = 1.2$ m^2/g) and alumina borosilicate fiberglass leached at 20°C for 30 min (support EB; $S_{sp} = 20$ m^2/g). The former support exhibited a low specific surface area and a specific pseudolayer structure, which is responsible for the intercalation of cations into narrow interlayer microcavities [5]. Borosilicate fiberglass undergoes degradation at a high degree of leaching; therefore, it is unsuitable for use as a support. Alumina borosilicate fiberglass with a ~35% degree of leaching was used, which was characterized by a wide variety of pores (from mesopores 15–50 Å in diameter to microcavities smaller than 10 Å) [6]. For comparison, silica gel A with $S_{sp} = 10$ m^2/g was used, which was described in [5].

An active component (Pt or Pd) was introduced by impregnating fiberglass with solutions of H_2PtCl_6, $H_2[PdCl_4]$, and the ammine complexes of platinum and palladium, which were synthesized according to the published procedures [7, 8]. Several methods were used for preparing the samples. The table summarizes the test catalysts and the notation. In method 1, fiberglass was impregnated at room temperature; then, it was separated from the solution, dried at 110°C, calcined in air at 300°C for 2 h, and reduced in hydrogen at 300°C for 2 h. The total metal content was varied from 0.03 to 0.52%. In method 2, impregnation was performed at elevated temperatures; then, the samples were washed with deionized water to remove metal compounds weakly bound to the support and then dried and calcined as specified in method 1. In method 3, cesium cations were intercalated into a fiberglass support; then, the addition of an active component and the thermal treatment were performed as specified in method 2. The intercalated cesium could produce a pil-

Test catalysts

Sample	Preparation method	Support	Active component content, wt %
Pt catalysts			
1-EB-0.52Pt	1	EB	0.52% Pt
1-EB-0.52Pt*	1	EB	0.15% Pt
1-CB-0.22Pt	1	CB	0.22% Pt
1-CB-0.10Pt**	1	CB	0.10% Pt
1-CB-0.03Pt	1	CB	0.03% Pt
2-CB-0.01Pt	2	CB	0.01% Pt
3-CB-0.20Cs-0.01Pt	3	CB + 0.20% Cs	0.01% Pt + 0.20% Cs
1-A-0.32Pt	1	SiO_2(A)	0.32% Pt
Pd catalysts			
1-CB-0.3Pd	1	CB	0.30% Pd
1-CB-0.2Pd	1	CB	0.20% Pd
2-CB-0.01Pd	2	CB	0.01% Pd
2-CB-0.02Pd	2	CB	0.02% Pd
3-CB-0.01Cs-0.01Pd	3	CB + 0.01% Cs	0.01% Pd + 0.01% Cs
3-CB-0.20Cs-0.01Pd	3	CB + 0.20% Cs	0.01% Pd + 0.20% Cs
1-A-0.25Pd	1	SiO_2(A)	0.25% Pd

* Sample washed with aqua regia.

** Sample calcined at 650°C.

laring effect in the microcavities of leached fiberglass and, hence, facilitate the penetration of Pt and Pd species. Usually, the metal content of catalysts prepared by methods 2 and 3 was no higher than 0.03%.

The palladium content was determined by atomic absorption spectrometry on an AAS-1 instrument, and the platinum content was determined on a Baird ICP atomic emission spectrometer.

The morphology of catalysts was studied by TEM in combination with electron microdiffraction techniques on JEM-100CX (100 kV) and JEM-2010 (200 kV; line-to-line resolution of 1.4 Å) microscopes used for obtaining medium-magnification images and high-resolution micrographs, respectively. The samples for TEM studies were prepared using two procedures: without destroying glass fibers or with the use of mechanical grinding followed by suspending the powders in ethanol and by the ultrasonic dispersion of the suspensions. The former procedure allowed us to study the morphology and particle size of supported metals on the outer surface of fibers, and the latter, the state of metals in the bulk of the support fibers. In both cases, the samples were fixed in standard copper gauzes. Perforated carbon bases were used for obtaining high-resolution micrographs. Note that the temperature of radiation–thermal sample heating at commonly used electron-beam intensities was no higher than 100°C [9]. In a number of cases, increased electron-beam intensities were used for evaluating the effect of elevated temperatures on the samples.

The X-ray photoelectron spectra were measured on a VG ESCALAB HP electron spectrometer, which was calibrated against the binding energies of the Au$4f_{7/2}$ (84.0 eV) and Cu$2p_{3/2}$ (932.6 eV) core levels, using MgK_α radiation ($h\nu$ = 1253.6 eV). Catalyst samples were fixed in a sample holder using a two-sided adhesive tape. The charging effect, which appeared in the course of photoemission, was taken into account by the internal standard method; the Si$2p$ spectrum of the support with E_b = 103.3 eV was taken as an internal standard [10, 11]. The platinum-to-silicon and palladium-to-silicon atomic ratios (n_i/n_{Si}) were calculated based on measurements of the intensities of the correspond-

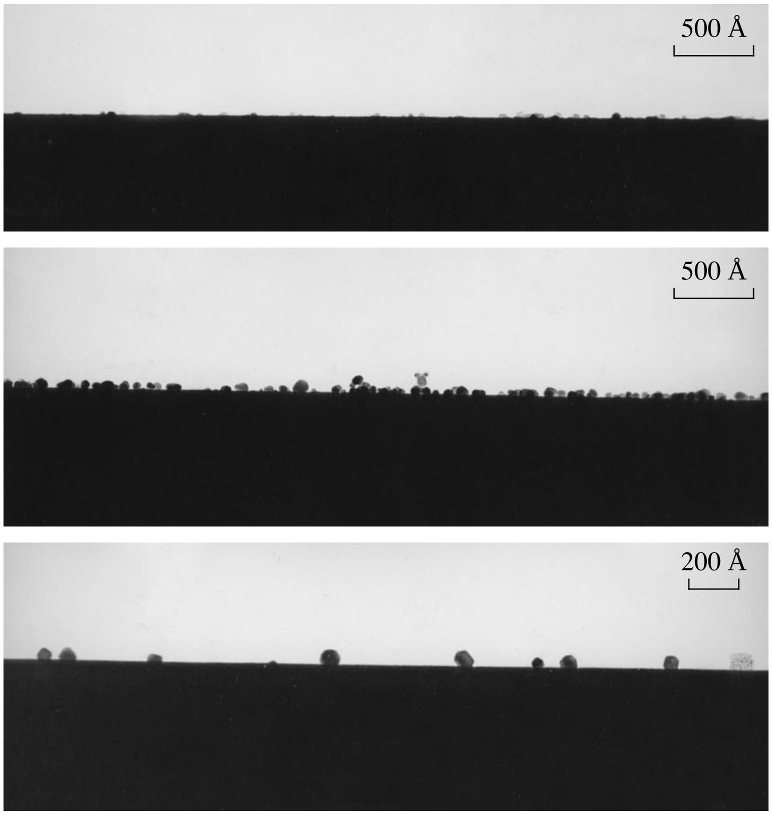

Fig. 1. Distribution of platinum particles over the outer surfaces of various fibers of a borosilicate support in the same sample 1-EB-0.52Pt according to TEM data.

ing XPS lines (I_i and I_{Si}) with the use of the following equation:

$$\frac{n_i}{n_{\mathrm{Si}}} = \frac{I_i/\mathrm{ASF}_i}{I_{\mathrm{Si}}/\mathrm{ASF}_{\mathrm{Si}}},$$

where ASF_i and $\mathrm{ASF}_{\mathrm{Si}}$ are the atomic sensitivity factors of the corresponding elements [10]. The layer-by-layer etching was performed using 2-keV argon ions at a current of 10 μA.

RESULTS

Morphology and Metal Distribution in Fiberglass Supports According to Electron Microscopy Data

(a) Distribution of metal particles on the outer surface of fiberglass. In catalysts prepared by method 1 (without washing off weakly bound metal compounds), metal particles of sizes ranging from several tens to hundreds of angstrom were detected on the outer surface of fibers in both of the fiberglass supports. For different fibers in the same sample, the surface coverage with platinum particles can vary from several particles over a 1000 × 1000 $Å^2$ surface element in a fiber to an almost complete monolayer of contacting particles or several layers in another fiber (Fig. 1). In a number of cases, platinum particle aggregates as branched dendrites or extended garlands of sizes up to 1 μm were observed.

Because the particle-size distribution is nonuniform, it is difficult to estimate the average particle size. However, it should be noted that the metal dispersity tends to decrease as the concentration and the temperature of calcination increase. Thus, in a soda–silica fiberglass support, the predominant particle size of platinum on the outer surface of fibers increased from 50 to 100 Å as the platinum content increased from 0.1 to 0.3 wt %. In sample 1-CB-0.10Pt, calcined at 650°C, particles with sizes up to 1000 Å were observed.

It is interesting that, in reference catalysts prepared by supporting Pt and Pd onto silica A with S_{sp} = 10 m^2/g, the metal particle size was higher than that on fiberglass supports with much lower S_{sp} of ~1 m^2/g. Thus, catalyst 1-A-0.25Pd exhibited a wide range of metal particle sizes from 50 to 300–500 Å.

In catalysts prepared by methods 2 and 3, no metal particles were detected on the outer surface of fiberglass.

(b) Distribution of metal particles in the mesopores of borosilicate fiberglass supports. The distribution of a metal within fibers depends on the structure peculiarities of these fibers. As found previously [6], pores 15–50 Å in diameter were formed in borosilicate

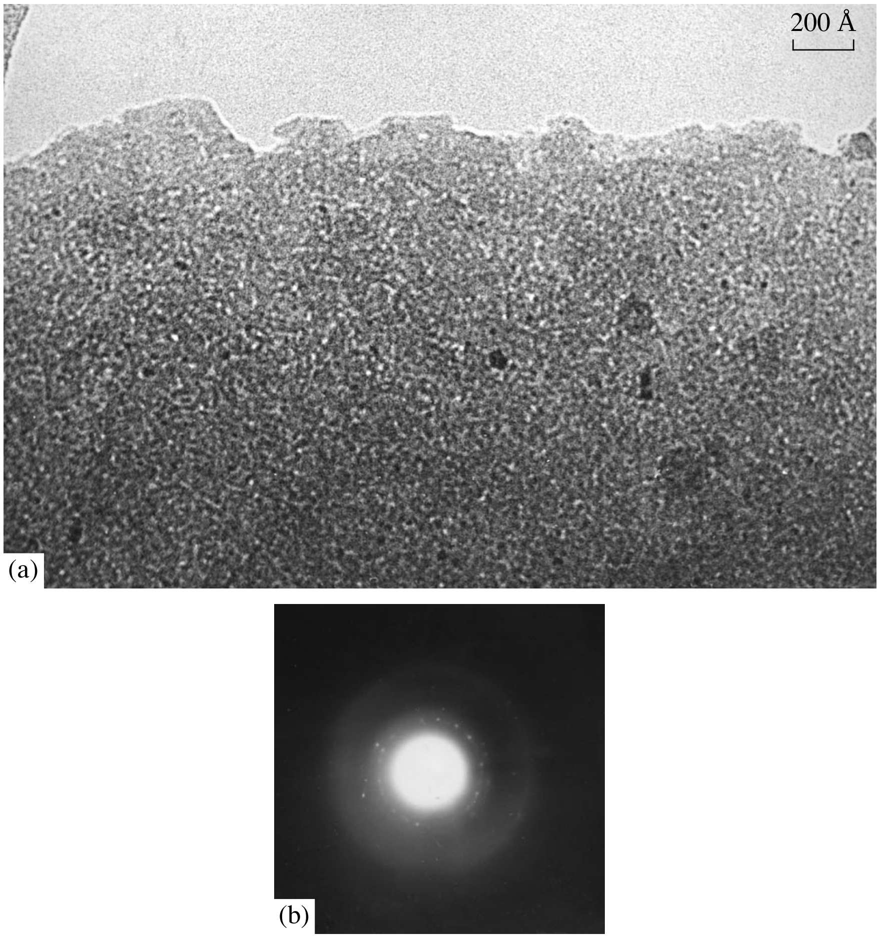

Fig. 2. (a) Distribution of platinum particles within the fibers of a borosilicate fiberglass support in catalyst 1-EB-0.52Pt and (b) microdiffraction on these particles.

glasses at medium degrees of leaching. These pores propagated from the outer surface into the fibers to a depth of several hundreds of angstrom. They are similar in adsorption properties to the mesopores of ordinary silica gels. Moreover, microcavities were present, which were analogous to those in pseudolayer soda–silica fiberglass [5].

In the study of Pt- and Pd-containing samples based on leached borosilicate fiberglass, the micrographs of fiber chips (Fig. 2) exhibited particles with sizes ranging from 15 to 100 Å (commensurable to the size of mesopores), and the diffraction pattern of these particles was characteristic of metals. Thus, a set of lines with interplanar spacings of 2.25, 1.95, 1.4, 1.2 Å, etc., is typical of platinum catalysts. Some of the chips contained no metal particles, probably because of the absence of a metal from the unleached central part of glass fibers.

The electron-beam heating did not significantly affect the particle size but the mesopores closed somewhat as a result of support sintering. This closure of pore openings can occur even in the course of catalyst preparation at the stage of thermal treatment at 300°C. It may result in the blocking (“encapsulation”) of metal particles by the pores by the support material. This was supported by the fact that about one-third of platinum (0.15%) was not extracted from sample 1-EB-0.52Pt (the table) upon the treatment with aqua regia. It is likely that closing and blocking an active component are most typical of supports based on B–Si fiberglass at low degrees of leaching. In this support, the presence of unleached constituents intensifies sintering even at comparatively low temperatures.

Note that particles ~10 Å in size additionally appeared in the bulk of fiberglass on heating. It is believed that, initially, along with mesoparticles, highly dispersed particles (smaller than 10 Å) were present in the sample, and they were localized in the microcavities of the support. In the initial state, these particles cannot be observed in micrographs because they are small and amorphous. Heating the electron beam resulted in the intense sintering of the smallest pores and in the agglomeration (coalescence) of metal microparticles in these pores.

As can be seen in high-resolution electron micrographs (Fig. 3), platinum particles in mesopores of

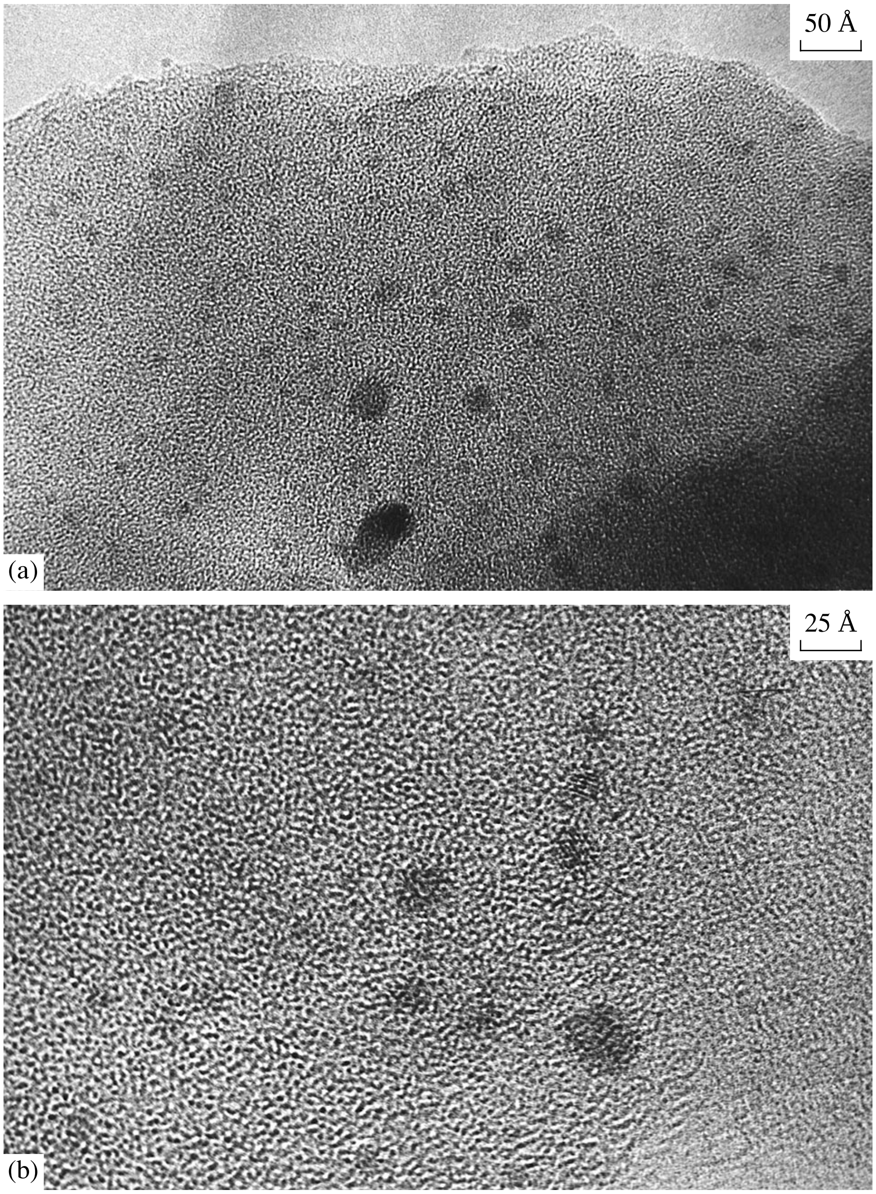

Fig. 3. TEM micrographs of sample 1-EB-0.52Pt after electron-beam heating: (a) magnification of 2×10^6 and (b) magnification of 4×10^6.

sizes larger than 10 Å occurred in the metallic state (d_{111} = 2.25 Å). For smaller particles localized in support microcavities, a pattern due to metal lattice planes was not observed. In this case, the absence of an fcc structure of the metal can be explained by the size effect. It is well known that icosahedral atomic configurations, which give no images of metal planes in high-resolution micrographs, are more typical of small platinum clusters.

Mesopores are absent from leached Na–Si fiberglass, and catalysts supported on them contained no mesoparticles analogous to those in borosilicate fiberglass supports.

(c) Distribution of Pt and Pd particles in the bulk of glass fibers. We found in preliminary catalytic experiments that catalysts based on Na–Si fiberglass prepared by methods 2 and 3 exhibited high catalytic activity, even though the metal content was low (0.01–0.02%). It was mentioned above that in these samples, metal particles were absent from the outer surface of fibers. Leached soda–silica fiberglass is characterized by a specific pseudolayer structure, which is responsible for the intercalation of rather large cations, such as Cs^+, into their bulk [5]. It was suggested that platinum and palladium ions can also be incorporated into the layered matrix of fiberglass, and they can occur there in a highly dispersed state. An electron-microscopic study

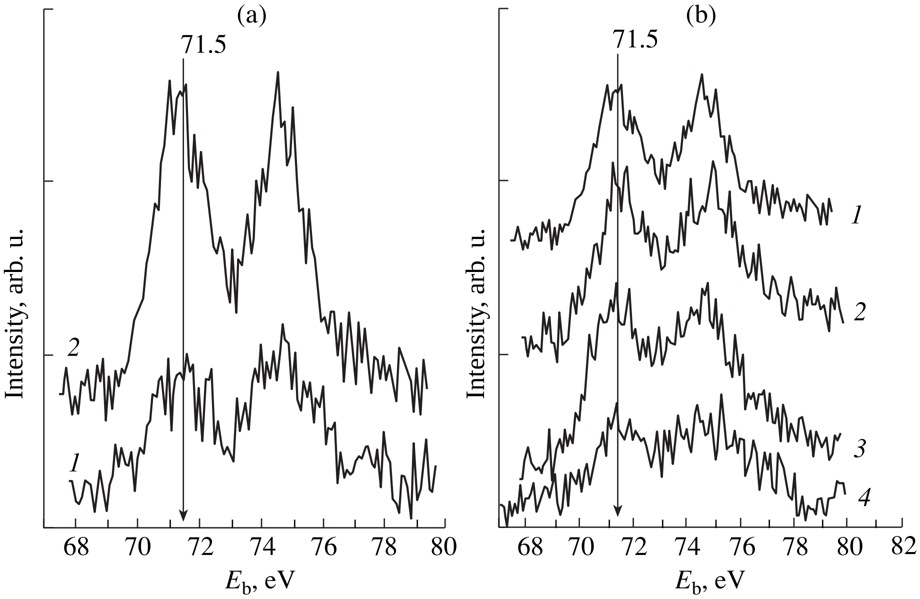

Fig. 4. (a) XPS spectra of the Pt4*f* core level for samples (*1*) 1-CB-0.10Pt and (*2*) 1-CB-0.22Pt. (b) Layer-by-layer ion etching of the surface of sample 1-CB-0.22Pt for (*1*) 0, (*2*) 1, (*3*) 4, and (*4*) 19 min.

of these low-concentration systems was quite difficult to perform, and metal particles within soda–silica fibers were not detected by direct observations. However, heating by an electron beam resulted in the appearance of microheterogeneity regions in the glass volume, and metal clusters of sizes up to 10 Å were observed in these regions by high-resolution electron microscopy. As in borosilicate supports, this can be explained by the fact that in the initial state, highly dispersed metal particles were present in the bulk of the fiberglass support. These metal particles manifested themselves only under the thermal action of an electron beam when they underwent agglomeration because of structural transformations in the support and an increase in the size of the microcavities.

XPS Study

The samples of Pt- and Pd-containing catalysts based on leached soda–silica fiberglass were studied by XPS.

The survey XPS spectra of all samples exhibited carbon lines (C1*s*) in addition to lines due to a support (Si2*p*, Si2*s*, O2*s*, and O1*s*) and a supported metal. The concentrations of carbon were found to be reasonably high (up to $n_c/n_{\mathrm{Si}} \sim 4$). The subsequent experiments on the argon ion etching of catalyst surfaces demonstrated that the C1*s* signal intensity dramatically decreased (by a factor of about 10) in just a few minutes of etching. This behavior is indicative of the surface localization of at least the major portion of carbon. Nevertheless, a considerable amount of carbon deposits was also detected in the surface layers of the catalysts (the stationary level in depth was no lower than $n_c/n_{\mathrm{Si}} \sim$ 0.3–0.4). This fact allowed us to suggest that the origin of carbon was of two kinds. First, hydrocarbon deposits adsorbed in the course of evacuating the spectrometer chamber with diffusion pumps are formed on the surface of samples. Second, it is most likely that carbon was introduced into the bulk at the stage of fiberglass preparation, for example, because of incomplete removal of oiling agent from fiberglass [5]. The binding energy of the C1*s* core level for adsorbed hydrocarbons (285.0 eV) [10] indicates that the charging effect was correctly taken into account using the XPS line of the support.

Figure 4 demonstrates the Pt4*f* core-level spectra measured for platinum-containing catalysts 1-CB-0.10Pt and 1-CB-0.22Pt prepared by method 1 and the spectra obtained by the layer-by-layer etching of the surface of sample 1-CB-0.22Pt. It can be seen that the position of the Pt4$f_{7/2}$ line is quite close to that of the bulk metallic state; the binding energy of the metallic state is lower by only 0.2–0.4 eV. This shift is considerably smaller than the shift detected in the oxidation of platinum (>1 eV); this fact is indicative of the metallic nature of particles. The observed shift is well known for small particles in supported systems. It can be explained either by a small deficiency in electron density on platinum particles, which results from the strong interaction of supported metal particles with defect regions on the SiO_2 surface (the effect of an initial state) or by the relaxation effect of a hole formed in the course of photoemission (the effect of a final state). The noticeable asymmetry on the side of lower values of E_b, which was detected for the Si2*p* core-level line, is indicative of the defect sites in the support, and it counts in favor of the former reason.

The quantitative data obtained from the XPS spectra of platinum and palladium demonstrated that the surface metal concentrations were much higher than the total metal content determined by chemical analysis. This fact indicates that the metal was primarily localized at the surface. For example, in sample 1-CB-0.03Pt prepared by method 1, the atomic fraction of platinum was found to be higher than the total metal concentration by almost one order of magnitude, as calculated from the XPS spectral intensities of all elements (calibrated using atomic sensitivity factors). An increase in the total platinum concentration by a factor of 7 (sample 1-CB-0.22Pt) did not result in a proportional increase in the surface concentration: as compared with sample 1-CB-0.03Pt, it increased by a factor of only 1.5. This is most likely due to an increase in the size of metal particles on the surface of fiberglass with increasing metal content. This conclusion was supported by data on the ion etching of the surface of sample 1-CB-0.22Pt (Fig. 4b). The spectral intensities were normalized to the intensity of the Si2*p* principal line of the support. It was found that in both of the samples, spectral lines did not completely disappear, even though the spectral intensities significantly decreased after 20-min etching. If we take into account that the rate of platinum and palladium sputtering under the etching conditions in use was 20–40 Å/min [12], the average sizes of metal particles can be estimated at 400–500 Å.

Note that the position of the Pt4*f* line remained unchanged in the course of etching, whereas a palladium catalyst exhibited a specific behavior. For the samples prepared by method 1, the value of E_b for Pd3$d_{5/2}$ (337.6 eV) was different from E_b for metallic palladium (335.6 eV). This fact indicates the existence of positively charged Pd ions. However, the Pd3$d_{5/2}$ line was significantly shifted toward lower binding energies even after 1-min etching, and the spectrum became identical to the spectrum of metallic palladium within another 3 min. This is indicative of the metallic nature of palladium within a supported particle and of the presence of an oxidized surface layer on the particle. The thickness of this surface layer can be estimated at 30–50 Å. This result is consistent with the well-known ability of palladium metal to undergo oxidation under exposure to oxygen.

Thus, method 1 for preparing catalysts primarily resulted in the localization of metal particles (conceivably, with an oxidized surface layer) on the outer surface of Na–Si fiberglass. The particle size increased with the concentration of introduced metals. Note that these conclusions are consistent with electron microscopy data.

It was interesting to examine the state of Pt and Pd in samples prepared by method 2. However, low metal concentrations (<0.03%), in particular, in the case of metal distribution throughout the bulk of fibers, presented problems in the XPS study of the state of metals because the line intensities were lower than the sensitivity level of XPS.

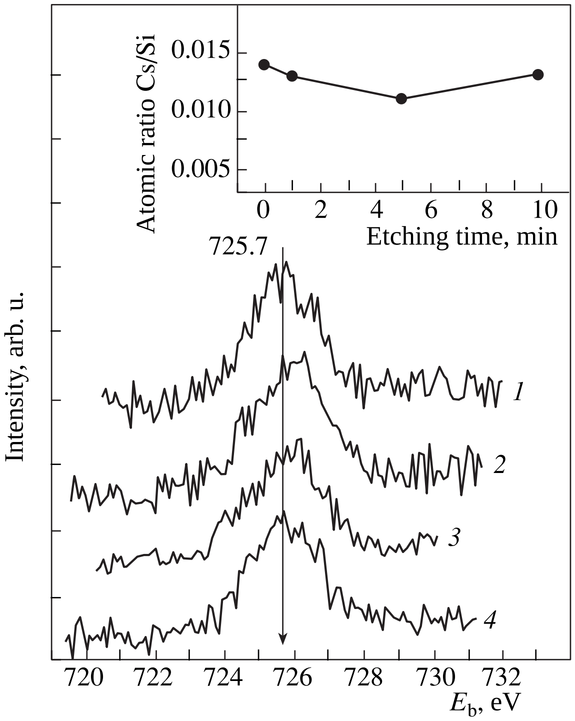

Fig. 5. XPS spectra of the Cs3*d* core level on the layer-by-layer ion etching of the CB + 0.2% Cs support for (*1*) 0, (*2*) 1, (*3*) 5, and (*4*) 10 min. The inset shows the Cs : Si atomic ratio as a function of etching time.

In this work, we examined the state of platinum and palladium in the bulk of fiberglass by XPS only in samples prepared by method 3 with cesium cations, which were preincorporated into fiberglass by ion exchange. As found previously [5], a comparatively bulky cation of cesium is intercalated into the interlayer microchannels of fiberglass, thus exerting a pillaring effect, which facilitates the subsequent penetration of other cations (Pt and Pd in our case) into these channels.

The successful intercalation of cesium into fiberglass was supported by data on the ion etching of a support modified with cesium (sample CB + 0.2% Cs). Figure 5 demonstrates both the XPS spectra of the Cs3*d* core level and the quantitative data on the Cs : Si atomic ratio as a function of etching time. It can be seen that the layer-by-layer etching did not considerably change both the position and the intensity of the Cs3*d* signal. This fact is indicative of a homogeneous distribution of cesium in the bulk of fibers at least to a depth of 50–100 Å. The chemical state of cesium also remained unchanged in the depth of the sample. The value of E_b for the Cs3$d_{5/2}$ line allows a conclusion on the occurrence of the singly charged ion Cs^+ [12]; it is likely that water molecules enter the first coordination sphere of this ion [13].

Figure 6 demonstrates the Pt4*f* and Pd3*d* core-level spectra, which were recorded in the course of the ion

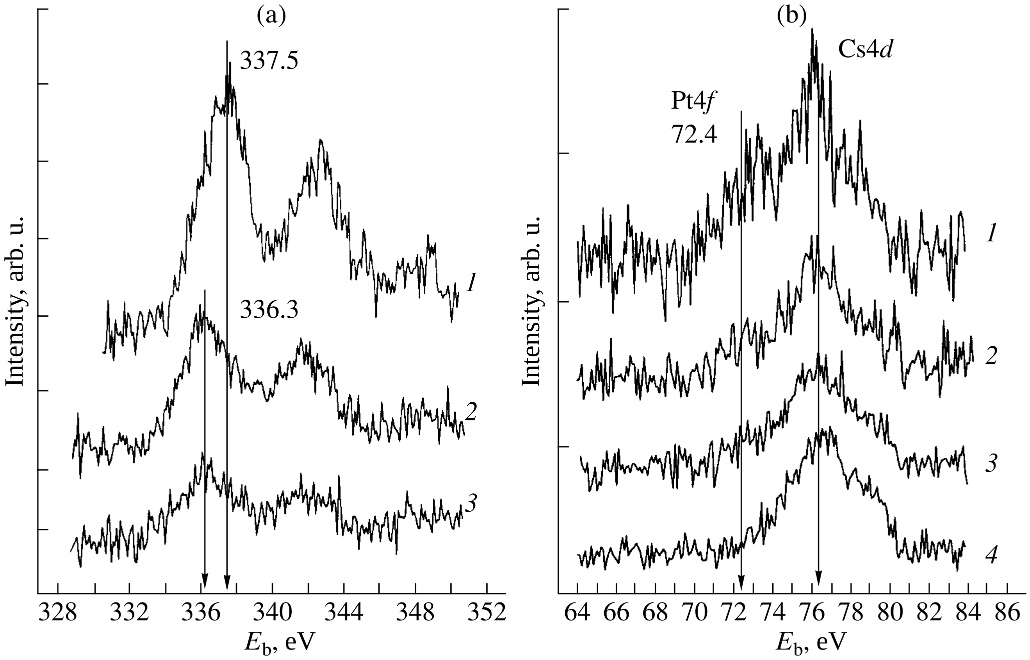

Fig. 6. XPS spectra of the Pd3*d* and Pt4*f* core levels on the layer-by-layer ion etching of (a) sample 3-CB-0.20Cs-0.01Pd for (*1*) 0, (*2*) 3, and (*3*) 13 min and (b) sample 3-CB-0.20Cs-0.01Pt for (*1*) 0, (*2*) 1, (*3*) 4, and (*4*) 9 min.

etching of samples 3-CB-0.20Cs-0.01Pd and 3-CB-0.20Cs-0.01Pt; palladium and platinum were introduced into the glass fibers by ion exchange after modifying the support with cesium. As in the case of samples prepared by method 1, the Pd3$d_{5/2}$ spectrum of sample 3-CB-0.20Cs-0.01Pd is characterized by a line with E_b = 337.5 eV. In the course of etching, this line was shifted toward lower binding energies, however, by only ~0.8 eV. This fact suggests that, in the bulk of the fibers, palladium occurs in a charged state rather than in the metallic state. A similar conclusion on the existence of positively charged platinum ions in Pt-containing catalyst 3-CB-0.20Cs-0.01Pt can be drawn from the Pt4*f* spectrum (Fig. 6b). Indeed, even though the Pt4*f* line and a region of cesium (Cs4*d*) overlap, it can be seen that the position of the platinum line (72.4 eV) is consistent with the published data for the Pt^{2+} ion, for example, in $Pt(OH)_2$ [10].

It can be seen in Fig. 6 that the XPS line intensities of platinum and palladium introduced into the bulk of fiberglass supports rapidly decreased and reached levels that cannot be measured by this technique. This conclusion can best be drawn from a comparison between quantitative data on the layer-by-layer analysis of samples prepared by methods 1 and 3 (Fig. 7). It can be seen that for platinum-containing sample 3-CB-0.20Cs-0.01Pt, which was prepared by method 3, the Pt4*f* signal disappeared even after 4-min etching; that is, the penetration depth of platinum into the bulk of fiberglass was no greater than 100 Å. In the case of similarly prepared palladium-containing sample 3-CB-0.20Cs-0.01Pd, the Pd3*d* line disappeared from the XPS spectrum at depths greater by a factor of two to three (Fig. 7a). In this case, the chemical state of palladium remained unchanged, suggesting that palladium introduced into fiberglass by method 3 occurs as positively charged ions. For samples 1-CB-0.22Pt and 1-CB-0.2Pd, which were prepared by method 1, an insignificant decrease in the intensities of Pd3*d* and Pt4*f* signals even after 20-min etching confirms the presence of coarse metal particles (up to 400 Å) on the surface of fibers.

DISCUSSION

The set of experimental data suggests that, in catalysts based on fiberglass materials, supported platinum and palladium occur in the following three forms:

(1) Metallic particles with sizes from tens to hundreds of angstrom are distributed over the outer surface of fibers; according to XPS and electron microscopy data, these particles are of a clearly defined metallic nature.

(2) In mesopores with sizes 15–100 Å, particles of commensurable sizes are localized; these particles exhibit a diffraction pattern typical of metals. This type of particle was observed in only leached B–Si fiberglass, which has a system of wider mesopores along with microcavities. An active component comparatively readily entered these pores even at the stage of impregnation, and it remained in them at the subsequent stages of calcination and reduction. In the course of thermal treatment at moderate temperatures, the localization sites of large metal particles remained

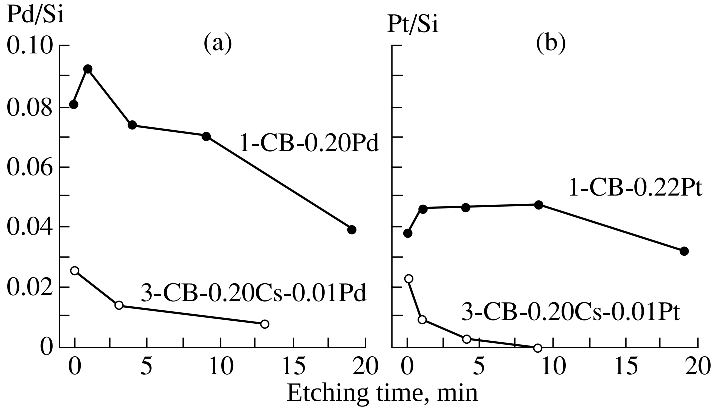

Fig. 7. Effects of the time of the ion etching of the surfaces of Pd and Pt catalysts prepared by different methods on the (a) Pd : Si and (b) Pt : Si atomic ratios.

unchanged. However, because of the thermal instability of incompletely leached borosilicate fibers, the mesopore close somewhat resulting in the blocking of a portion of the metal, which becomes unextractable with acids. Smaller pores and particles localized in the bulk of glass fibers can coalesce at elevated temperatures to increase in size.

(3) Metal ion species are localized in the bulk of fiberglass. Under certain preparation conditions, comparatively bulky cations can be intercalated into fiberglass because of the mobility of thin silica walls of microcavities by these cations. The amount of a metal and the depth of its penetration into the bulk of fiberglass can be controlled by preparation conditions and by the introduction of cointercalates, which cause pillaring effects [6, 14].

It is evident that the production of highly dispersed particles of active components is most important for the manufacture of active catalysts with low concentrations of active components. This problem is particularly topical for expensive noble metals. It is well known that the stabilization of supported metals in a highly dispersed state (up to 10 Å) is very difficult to perform. Supports with high specific surface areas (>200 m^2/g) and special preparation techniques that provide the homogeneous and strong immobilization of active component precursors on the surface are commonly used for this purpose. For example, it was found that superfine initial particles can be obtained by supporting organometallic Pt and Pd compounds onto highly dispersed silica or alumina [15, 16]. However, being localized on a surface these particles are unstable, and they readily undergo aggregation at the thermal stages of synthesis and in the course of operation.

In this work, we found that highly dispersed Pt and Pd particles can be obtained on supports having very low specific surface areas (~1 m^2/g); this is due to the structure peculiarities of the supports. In leached soda–silica fiberglass supports with pseudolayer intercalation structures [5], highly dispersed metal particles are fixed in the bulk rather than on the surface of fiberglass under certain preparation conditions; this is due to the fact that cations penetrate into interlayer spaces as deep as 100 Å. Each of these microcavities is connected with the outer surface of the fiber; however, it is likely that a microcavity is unconnected with a neighboring one (separated from them with silicon–oxygen layers). The localization of particles inside fiberglass makes the particle growth more difficult as compared with particles supported on the outer surface. Thus, in spite of a very low specific surface area, soda–silica fiberglass supports can stabilize highly dispersed particles of a supported metal. Note that, even though the amount of a metal intercalated into fiberglass is small (<0.03%) because the metal shallowly penetrates into the bulk, the metal concentration in the surface layers of fiberglass can be higher than the total concentration by one or two orders of magnitude. It is also believed that highly dispersed Pt and Pd species that are localized in the microcavities of a fiberglass matrix occur in a metastable state and can exhibit high catalytic activity. At the same time, localization in the bulk of fiberglass can result in steric hindrances for the substrates of a catalytic reaction. Evidently, the difficulties associated with transport significantly depend on the reaction conditions and substrate properties. Moreover, intercalated particles exert a pillaring effect to move apart from the walls of microcavities and, hence, to facilitate the transport of gaseous reactants.

In conclusion, note that the above experiments were mainly performed with freshly reduced catalysts. It is well known that the initial state of an active component can be changed in the course of catalytic tests. Depending on the specific conditions of a catalytic reaction, the activity can either increase or decrease because of this change. In this work, we did not specifically study the evolution of catalysts under reaction conditions. However, in the testing of Pt- and Pd-containing catalysts in propane oxidation, we found no detectable changes in the catalytic activity after catalyst operation for several hundreds of hours at temperatures up to 500°C. In the reaction of SO_2 oxidation, a platinum catalyst (~0.02% Pt on soda–silica fiberglass) was stable in operation for ~100 h at 700°C. This leads us to believe that the initial state of the catalyst remained unchanged in the test reactions; in any case, the degree to which the state of the catalyst may be changed had no effect on the catalytic properties.

ACKNOWLEDGMENTS

This work was supported in part by the NATO Science Foundation “Science for Peace” (project no. SfP-971897). We are grateful to L.A. Sergeeva for performing chemical analysis.

REFERENCES

1. Nicholas, D.M., Shah, Y.T., and Zlochower, I.A., *Ind. Eng. Chem., Prod. Res. Dev.*, 1976, vol. 15, no. 1, p. 29.
2. Barelko, V.V., Khalzov, P.I., Zviagin, V.N., and Onischenko, V.Ya., *Proc. 11 Conf. “Modern Trends in Chemical Kinedtics and Catalysis,” Novosibirsk*, 1995, vol. 2(1), p. 164.
3. Barelko, V.V., Yuranov, I.A., Cherashev, A.V., *et al.*, *Dokl. Ross. Akad. Nauk*, 1998, vol. 361, no. 4, p. 485.
4. Kiwi-Minsker, L., Yuranov, I., Holler, V., and Renken, A., *Chem. Eng. Sci.*, 1999, vol. 54, p. 4785.
5. Simonova, L.G., Barelko, V.V., Lapina, O.B., *et al.*, *Kinet. Katal.*, (in press).
6. Simonova, L.G., Barelko, V.V., Paukshtis, E.A., *et al.*, *Kinet. Katal.*, 2001, vol. 42, no. 6, p. 907 (*Kinet. Catal.* (Engl. transl.), 2001, vol. 42, no. 6, p. 828).
7. Boronin, V.S., Nikulin, V.S., and Poltorak, O.M., *Zh. Fiz. Khim.*, 1963, vol. 37, no. 5, p. 1174.
8. *Handbuch der praparativen anorganischen Chemie*, Brauer, G., Ed., Stuttgart: Enke, 1978, vol. 5, p. 1805.
9. Reimer, L., *Transmission Electron Microscopy*, Berlin: Springer, 1984, p. 421.
10. *Practical Surface Analysis*, Briggs, D. and Seah, M.P., Eds., New York: Wiley, 1990, vol. 1.
11. Wagner, C.D., Riggs, W.M., Davis, L.E., Moulder, J.F., and Muilenberg, G.E., *Handbook of X-Ray Photoetectron Spectroscopy*, Perkin-Elmer, MN, 1979.
12. Ebbinghaus, G. and Simon, A., *Chem. Phys.*, 1970, vol. 43, p. 117.
13. Bukhtiyarov, V.I., Prosvirin, I.P., Kvon, R.I., *et al.*, *Appl. Surf. Sci.*, 1997, vol. 115, p. 135.
14. Vaughan, D.E.W., *Catal. Today*, 1988, vol. 2, nos. 2–3, p. 297.
15. Yermakov, Yu.I., *Catal. Rev.–Sci. Eng.*, 1976, vol. 13(1), p. 77.
16. Ryndin, Yu.A., *Cand. Sci. (Chem.) Dissertation*, Novosibirsk: Inst. of Catalysis, 1977.